

Appendix C. Diagnostic Results for High-Flow Event Simulations

As discussed in Section 3.2, bed shear stress distributions in the LDW were evaluated for these flow conditions: 1) average (mean) flow (1,340 cfs); 2) 2-yr high-flow event (8,400 cfs); 3) 10-yr high-flow event (10,800 cfs); and 4) 100-yr high-flow event (12,000 cfs). The effects of neap and spring tidal cycles on bed shear stress were also considered. The incoming or rising tide is traditionally referred to as the flood tide because it floods the channel. The outgoing tide is referred to as the ebb tide. The strength of the ebb and flood tide velocities varies diurnally and over spring and neap cycles. Simulation results indicate that in general, ebb tide bed shear stresses are higher than during flood tide in the region upstream of the saltwater wedge. Downstream of the saltwater wedge, tidal distortion in shallow estuaries leads to the flood tide having a shorter duration than the ebb tide. As a consequence, the peak flood tide velocities, and therefore bed shear stresses, generally tend to be greater than the peak ebb tide velocities. The model may be used to predict the extent of the differences between ebb and flood tide velocities and whether or not those differences are significant with respect to the potential for bed scour.

As discussed in Section 3.2, areas within which the critical shear stress is exceeded (i.e., initial erosion rate of 10^{-4} cm/s or greater) for a range of high-flow and tidal conditions are estimated by comparing predicted bed shear stress distributions to surface-layer τ_{cr} , which is set at 0.16 Pa based on the results of the Sedflume data analysis. Excess shear stress (τ_{ex}) represents the difference between bed shear stress and critical shear stress (i.e., $\tau_{ex} = \tau - \tau_{cr}$). This quantity provides a measure of the potential for bed scour, with erosion rate increasing as excess shear stress increases. Analyzing the spatial distributions of τ_{ex} aids in refining the critical shear analysis, discussed above, by identifying areas of low and high excess shear stress. This information is used to develop inferences concerning potential bed scour in various reaches of the LDW; areas of relatively low bed scour can be differentiated from areas of relatively high bed scour.

Spatial distributions of critical shear stress exceedance during average-flow conditions for a range of tidal conditions are presented in Figures C-1 through C-4. These results show that the critical shear stress is exceeded in a relatively small area in the upper turning basin (i.e., approximately RM 4.6). Thus, negligible erosion, relative to a high-flow event, is predicted to occur in the LDW during average-flow conditions.

Spatial distributions of critical shear stress exceedance during a 2-yr high-flow event for a range of tidal conditions are presented in Figures C-5 through C-8. Within Reach 1 (downstream of RM 2.0), only two relatively small areas (i.e., near RM 0.8 and RM 2.0) are predicted to exceed the critical shear stress during this high-flow event. In Reaches 2 and 3 (upstream of RM 2.0), the critical shear is exceeded in most of the

navigation channel and portions of the bench areas, with areas near the shoreline generally experiencing negligible potential erosion.

Excess shear stress distributions for the 2-yr high-flow event are shown in Figures C-9 through C-12. Downstream of RM 2.0 (Reach 1), τ_{ex} values are 0.2 Pa or less. In Reaches 2 and 3, the highest τ_{ex} values occur in the navigation channel, with values of 1 Pa or less downstream of RM 4.6. Higher values (i.e., greater than 1.5 Pa) occur in a small area in the upper turning basin near RM 4.7. In the bench areas of Reach 2 and 3, excess shear stress values are 1 Pa or less.

Spatial distributions of critical shear stress exceedance during a 10-yr high-flow event for a range of tidal conditions are presented in Figures C-13 through C-16. Within Reach 1 (downstream of RM 2.0), the critical shear stress is exceeded between RM 1.9 and 2.0, and within two relatively small areas in the center portion of channel downstream of RM 0.9. In Reaches 2 and 3 (upstream of RM 2.0), the critical shear is exceeded in most of the navigation channel and large portions of the bench areas.

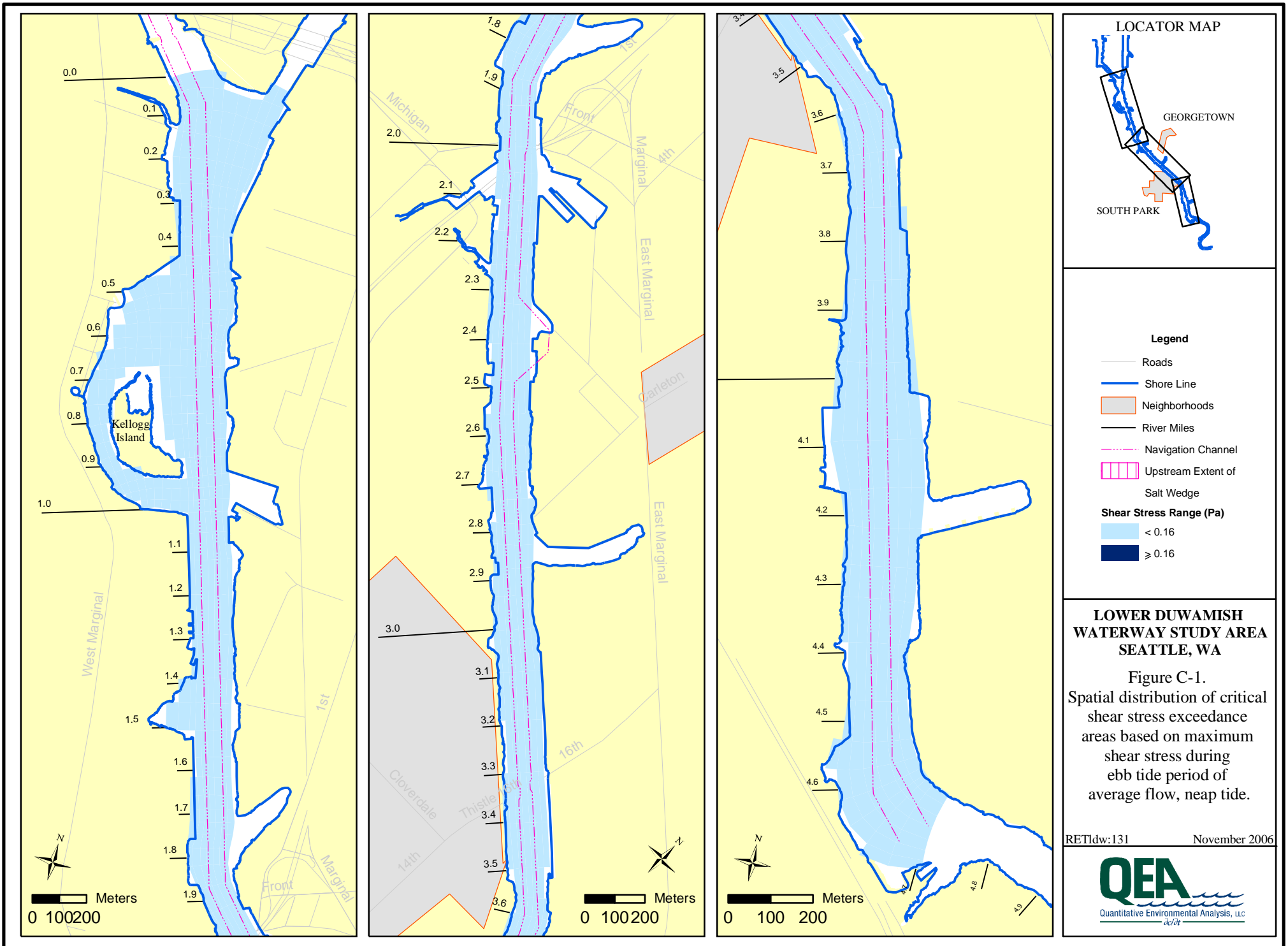
Excess shear stress distributions for the 10-yr high-flow event are shown in Figures C-17 through C-20. Downstream of RM 2.0 (Reach 1), τ_{ex} values are 0.2 Pa or less. In Reaches 2 and 3, excess shear stress values are typically higher during the 10-yr event than during the 2-yr event, as might be expected. The highest τ_{ex} values occur in the navigation channel, with values of 1.5 Pa or less downstream of RM 4.6. Higher values (i.e., greater than 1.5 Pa) occur in a small area in the upper turning basin near RM 4.7. In the bench areas of Reach 2 and 3, excess shear stress values are 1 Pa or less.

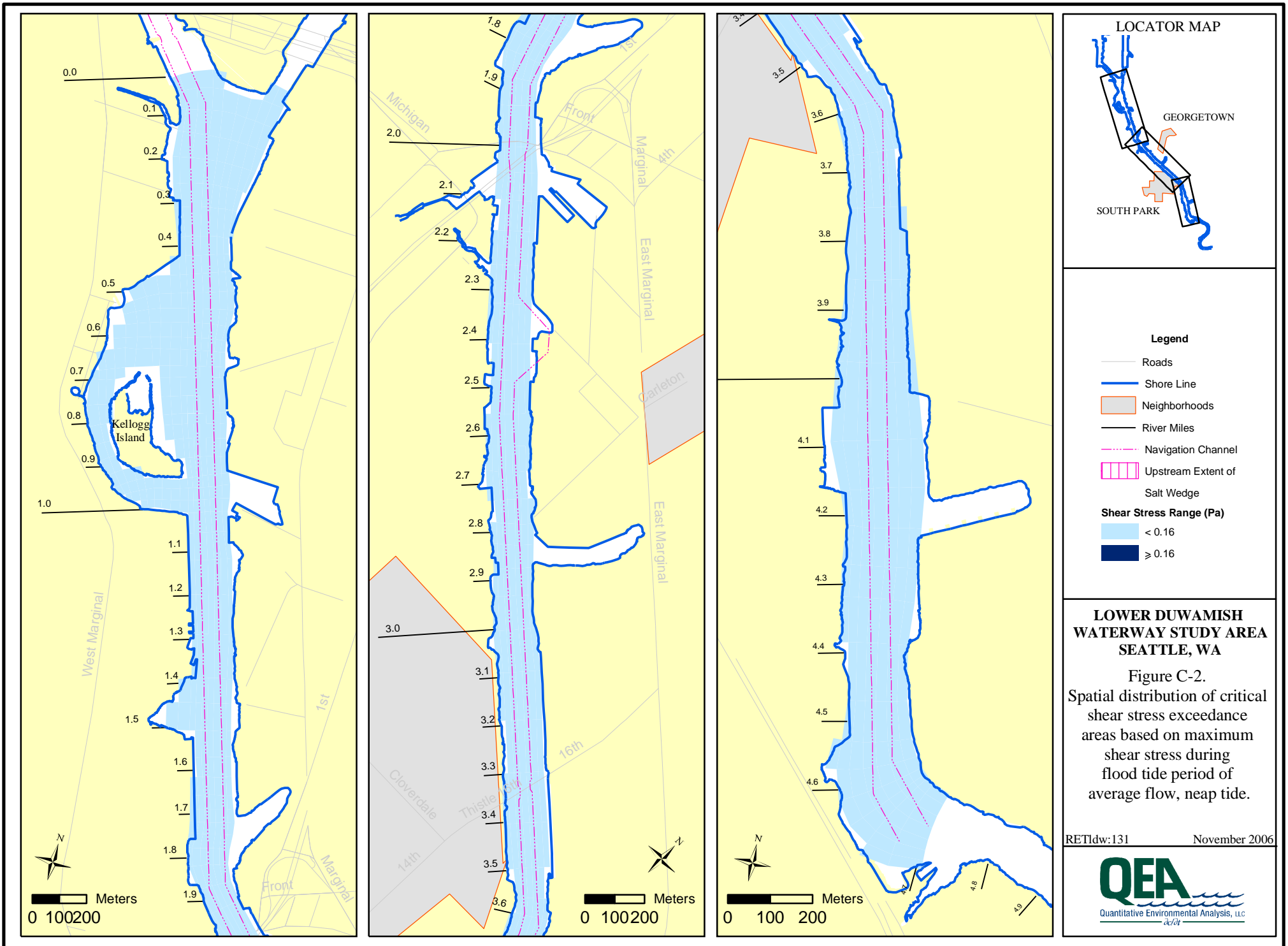
Results for the 100-yr high-flow event during spring tide conditions were presented in Section 3.2. For completeness, the results for the neap tide conditions during this event are presented here. Critical shear stress exceedance distributions are shown in Figures C-21 and C-22. Excess shear stress distributions are presented in Figures C-23 and C-24. Consistent with differences between neap and spring tide conditions for the 2-yr and 10-yr high-flow events, predicted shear stresses for neap tide during a 100-yr high-flow event are generally lower than for spring tide conditions.

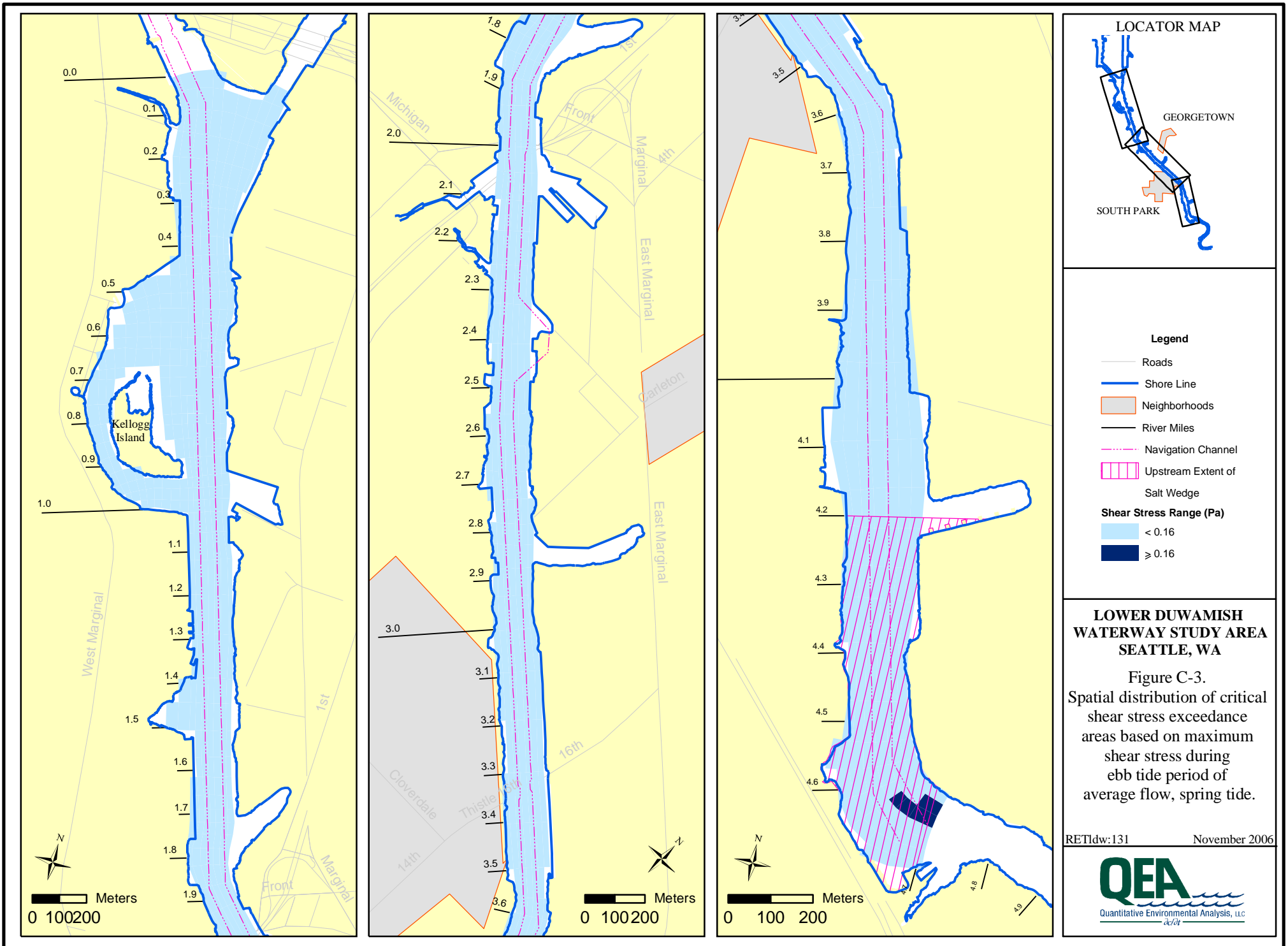
LIST OF FIGURES CITED IN APPENDIX C

- Figure C-1. *Spatial distribution of critical shear stress exceedance areas based on maximum shear stress during ebb tide period of average flow, neap tide*
- Figure C-2. *Spatial distribution of critical shear stress exceedance areas based on maximum shear stress during flood tide period of average flow, neap tide*
- Figure C-3. *Spatial distribution of critical shear stress exceedance areas based on maximum shear stress during ebb tide period of average flow, spring tide*
- Figure C-4. *Spatial distribution of critical shear stress exceedance areas based on maximum shear stress during flood tide period of average flow, spring tide*
- Figure C-5. *Spatial distribution of critical shear stress exceedance areas based on maximum shear stress during ebb tide period of 2-yr high-flow event, neap tide*
- Figure C-6. *Spatial distribution of critical shear stress exceedance areas based on maximum shear stress during flood tide period of 2-yr high-flow event, neap tide*
- Figure C-7. *Spatial distribution of critical shear stress exceedance areas based on maximum shear stress during ebb tide period of 2-yr high-flow event, spring tide*
- Figure C-8. *Spatial distribution of critical shear stress exceedance areas based on maximum shear stress during flood tide period of 2-yr high-flow event, spring tide*
- Figure C-9. *Spatial distribution of excess shear stress based on maximum shear stress during ebb tide period of 2-yr high-flow event, neap tide*
- Figure C-10. *Spatial distribution of excess shear stress based on maximum shear stress during flood tide period of 2-yr high-flow event, neap tide*
- Figure C-11. *Spatial distribution of excess shear stress based on maximum shear stress during ebb tide period of 2-yr high-flow event, spring tide*
- Figure C-12. *Spatial distribution of excess shear stress based on maximum shear stress during flood tide period of 2-yr high-flow event, spring tide*
- Figure C-13. *Spatial distribution of critical shear stress exceedance areas based on maximum shear stress during ebb tide period of 10-yr high-flow event, neap tide*
- Figure C-14. *Spatial distribution of critical shear stress exceedance areas based on maximum shear stress during flood tide period of 10-yr high-flow event, neap tide*
- Figure C-15. *Spatial distribution of critical shear stress exceedance areas based on maximum shear stress during ebb tide period of 10-yr high-flow event, spring tide*
- Figure C-16. *Spatial distribution of critical shear stress exceedance areas based on maximum shear stress during flood tide period of 10-yr high-flow event, spring tide*
- Figure C-17. *Spatial distribution of excess shear stress based on maximum shear stress during ebb tide period of 10-yr high-flow event, neap tide*

- Figure C-18. Spatial distribution of excess shear stress based on maximum shear stress during flood tide period of 10-yr high-flow event, neap tide*
- Figure C-19. Spatial distribution of excess shear stress based on maximum shear stress during ebb tide period of 10-yr high-flow event, spring tide*
- Figure C-20. Spatial distribution of excess shear stress based on maximum shear stress during flood tide period of 10-yr high-flow event, spring tide*
- Figure C-21. Spatial distribution of critical shear stress exceedance areas based on maximum shear stress during ebb tide period of 100-yr high-flow event, neap tide*
- Figure C-22. Spatial distribution of critical shear stress exceedance areas based on maximum shear stress during flood tide period of 100-yr high-flow event, neap tide*
- Figure C-23. Spatial distribution of excess shear stress based on maximum shear stress during ebb tide period of 100-yr high-flow event, neap tide*
- Figure C-24. Spatial distribution of excess shear stress based on maximum shear stress during flood tide period of 100-yr high-flow event, neap tide*





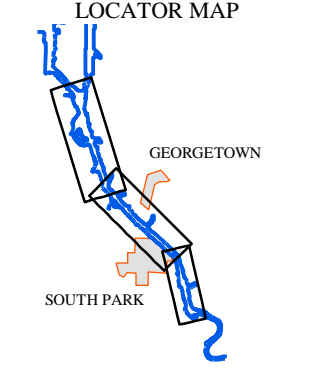
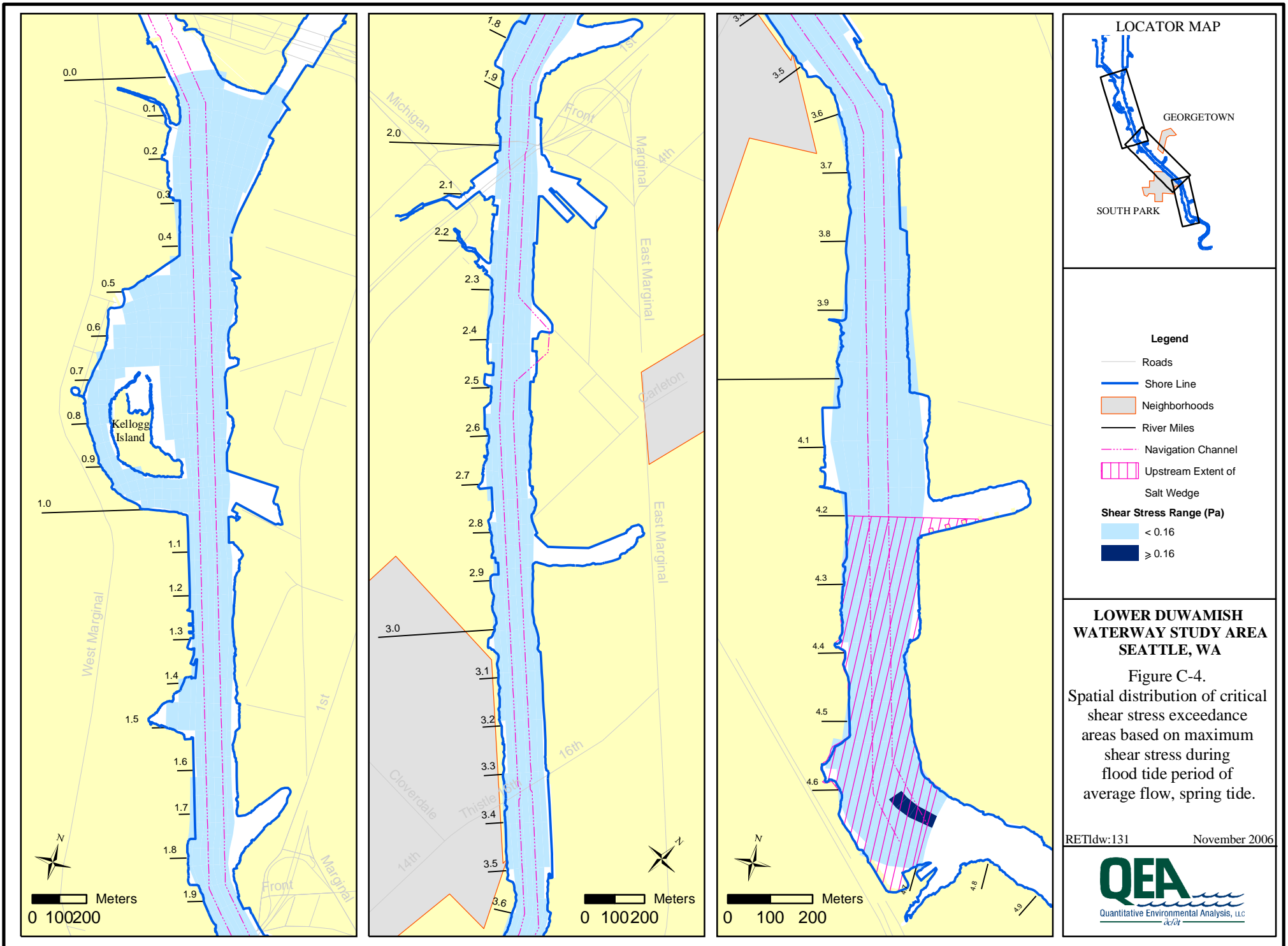


**LOWER DUWAMISH
WATERWAY STUDY AREA
SEATTLE, WA**

Figure C-3.
Spatial distribution of critical
shear stress exceedance
areas based on maximum
shear stress during
ebb tide period of
average flow, spring tide.

RETIdw:131 November 2006





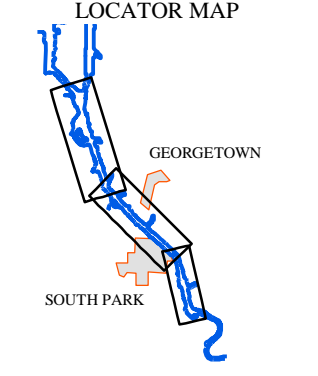
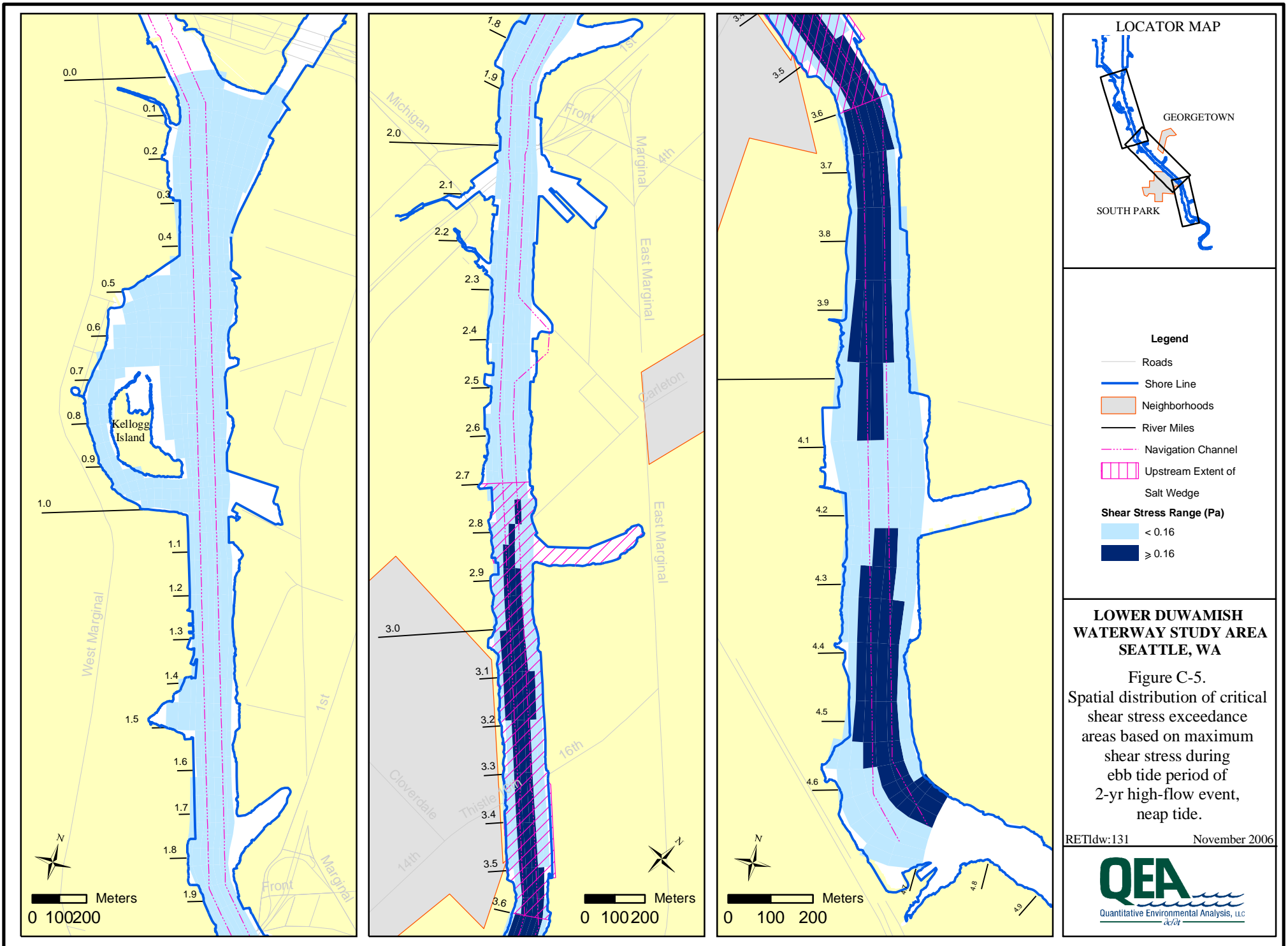
- Legend**
- Roads
 - Shore Line
 - Neighborhoods
 - River Miles
 - Navigation Channel
 - Upstream Extent of Salt Wedge
- Shear Stress Range (Pa)**
- <math>< 0.16</math>
 - ≥ 0.16

LOWER DUWAMISH WATERWAY STUDY AREA SEATTLE, WA

Figure C-4. Spatial distribution of critical shear stress exceedance areas based on maximum shear stress during flood tide period of average flow, spring tide.

RETIdw:131 November 2006





Legend

- Roads
- Shore Line
- ▭ Neighborhoods
- River Miles
- Navigation Channel
- ▭ Upstream Extent of Salt Wedge

Shear Stress Range (Pa)

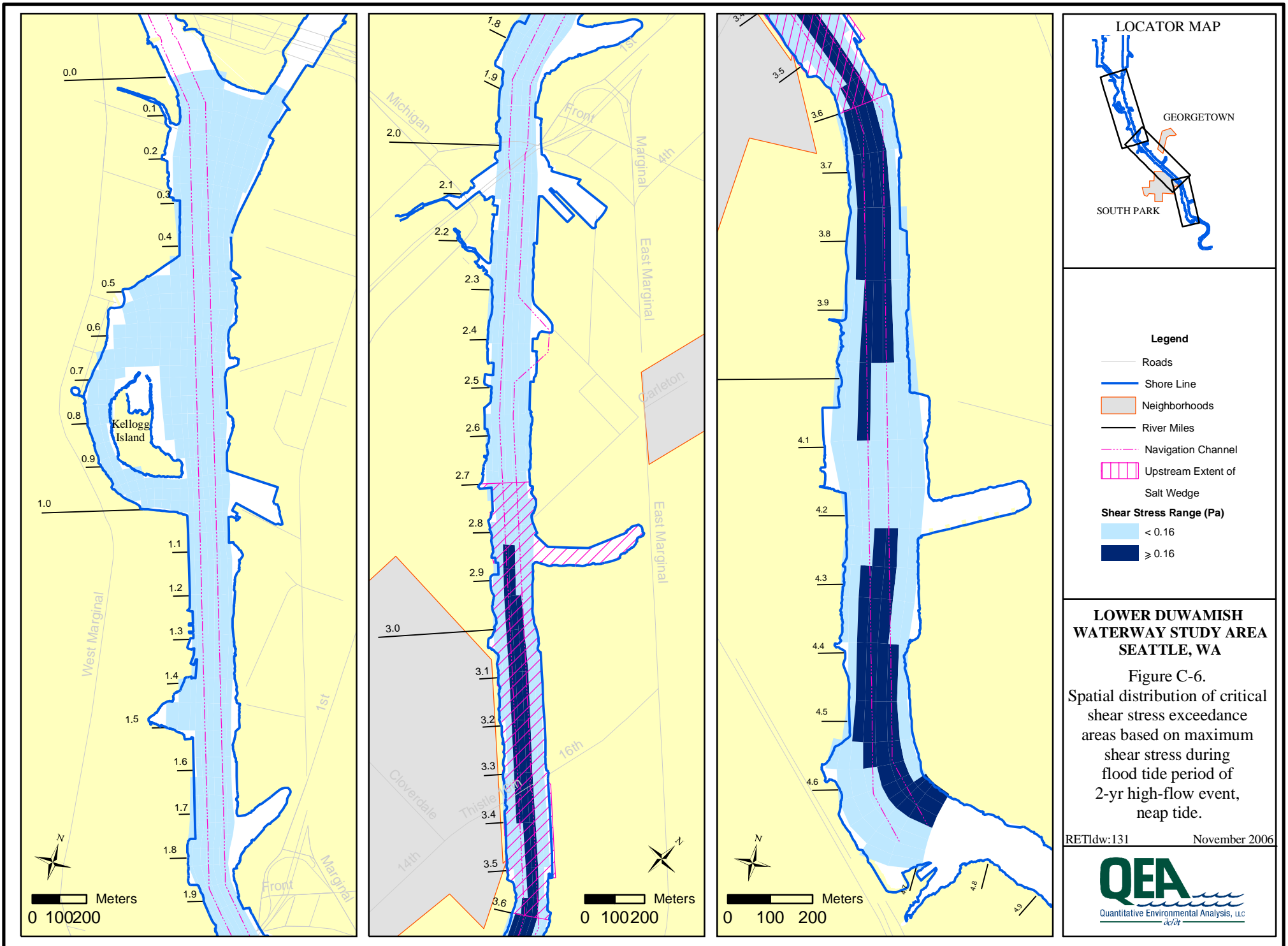
- ▭ < 0.16
- ▭ ≥ 0.16

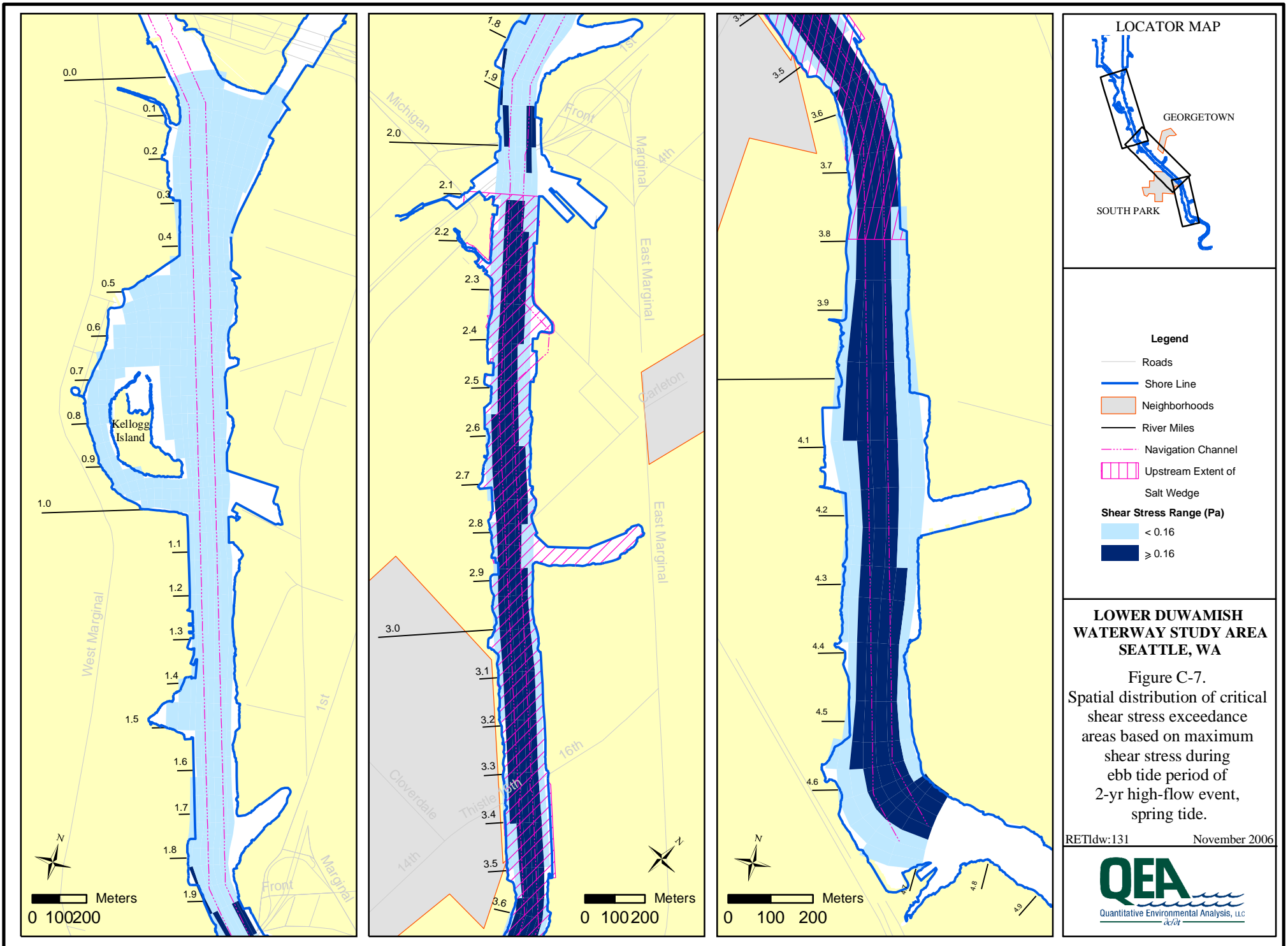
LOWER DUWAMISH WATERWAY STUDY AREA SEATTLE, WA

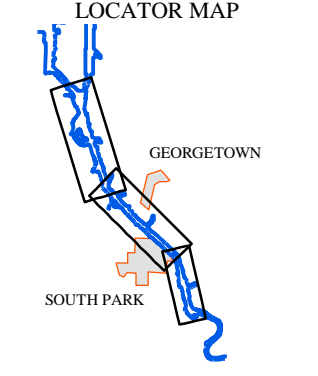
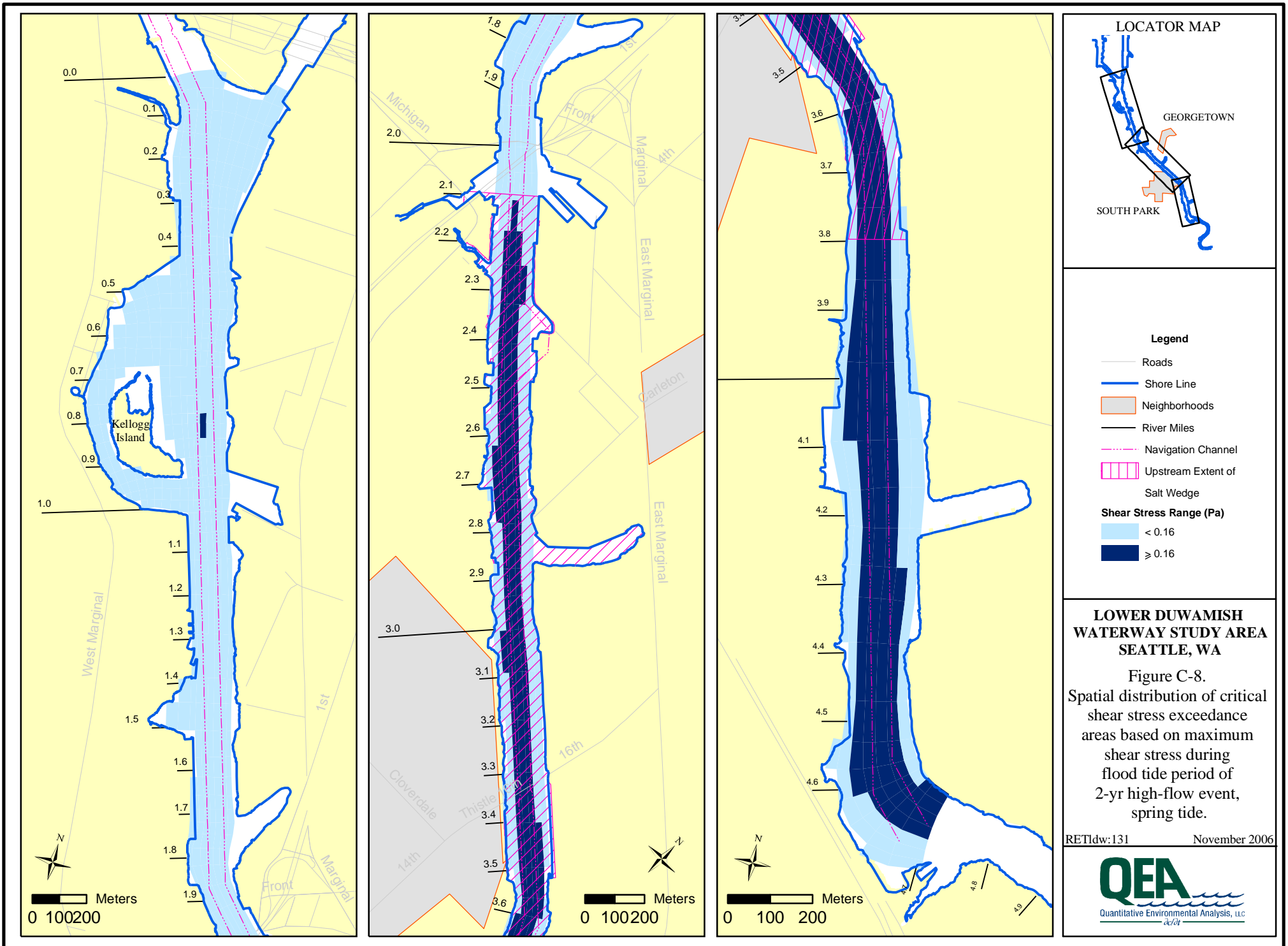
Figure C-5. Spatial distribution of critical shear stress exceedance areas based on maximum shear stress during ebb tide period of 2-yr high-flow event, neap tide.

RETIdw:131 November 2006









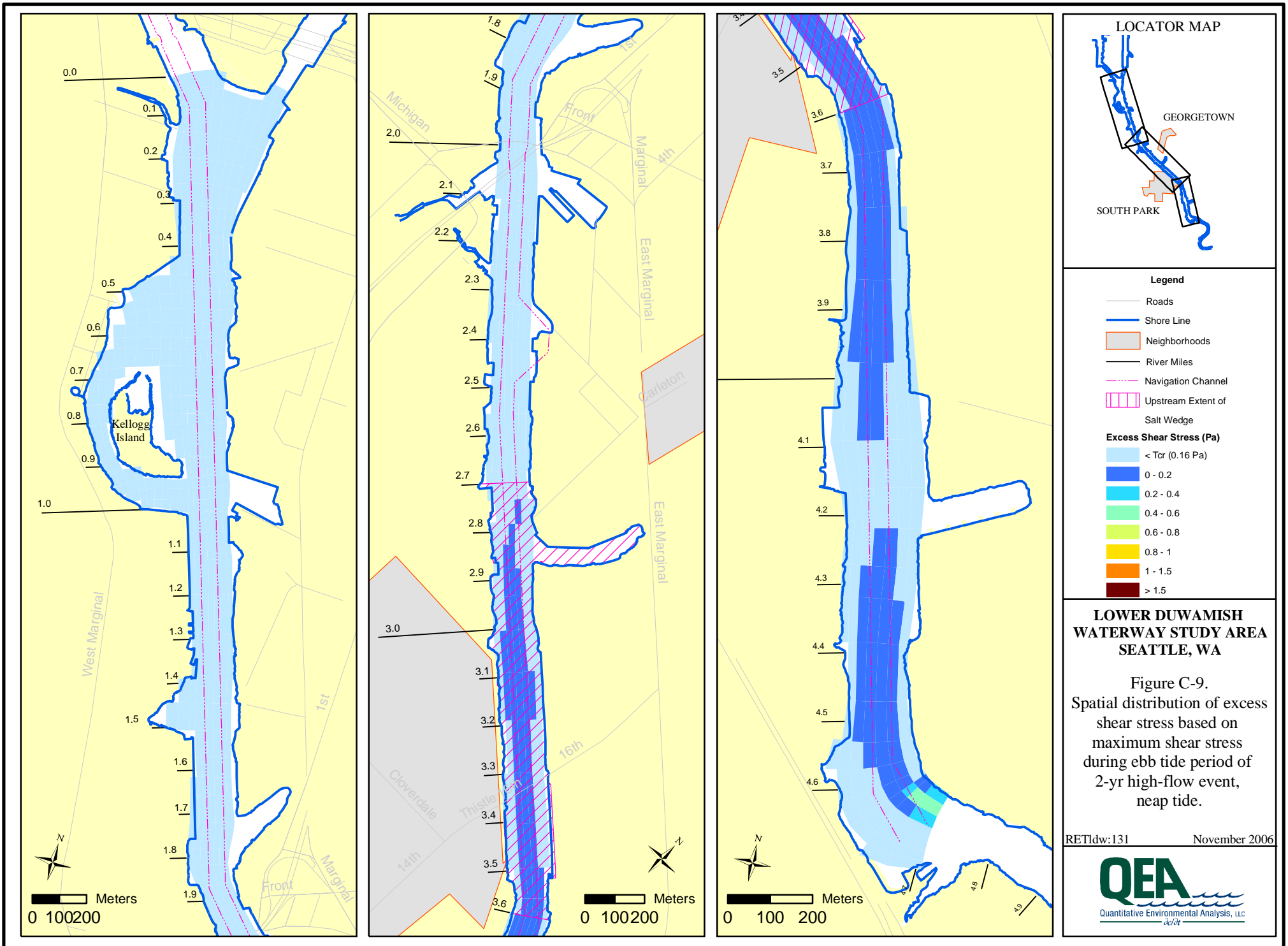
- Legend**
- Roads
 - Shore Line
 - Neighborhoods
 - River Miles
 - Navigation Channel
 - Upstream Extent of Salt Wedge
- Shear Stress Range (Pa)**
- < 0.16
 - ≥ 0.16

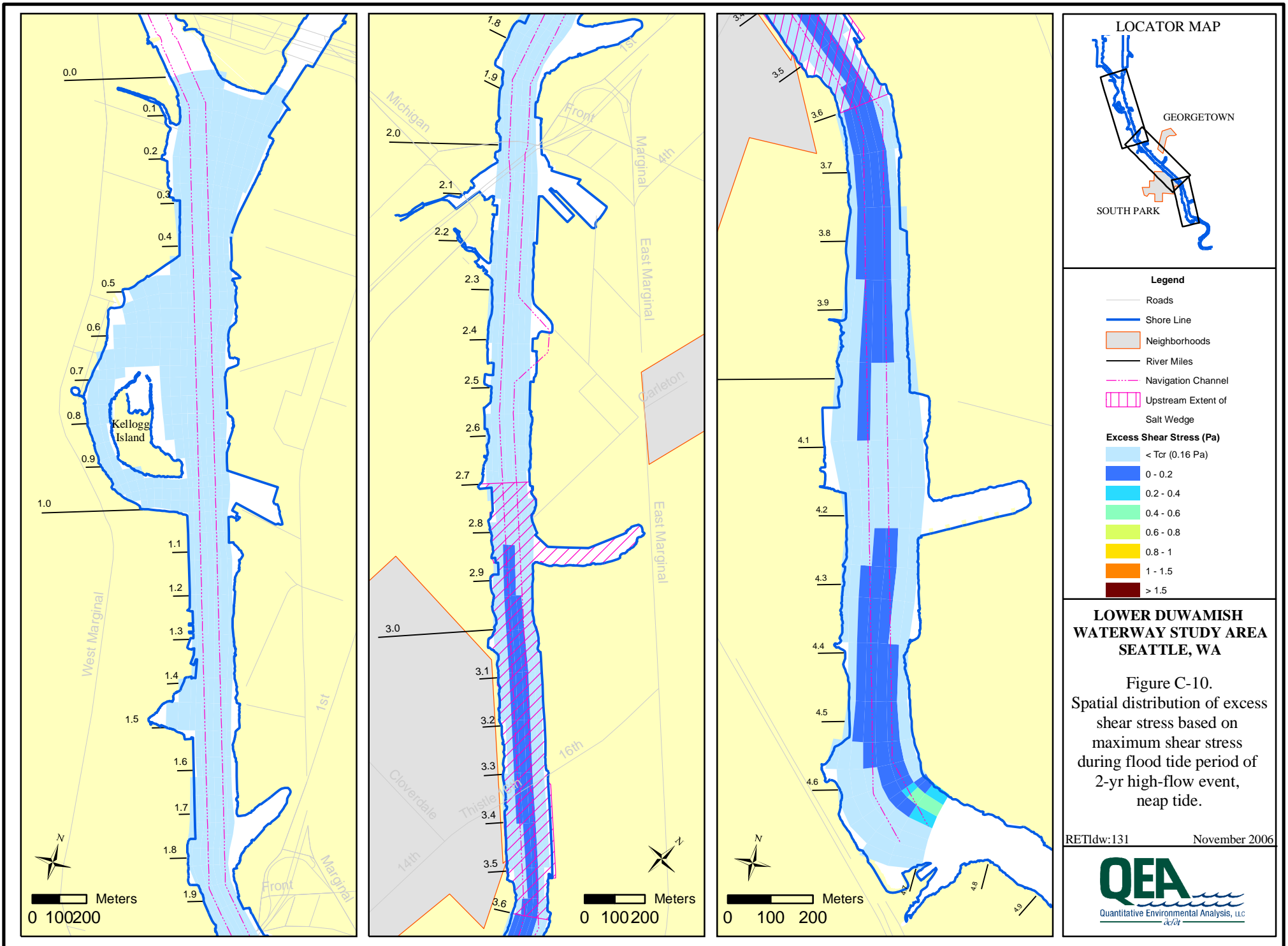
LOWER DUWAMISH WATERWAY STUDY AREA SEATTLE, WA

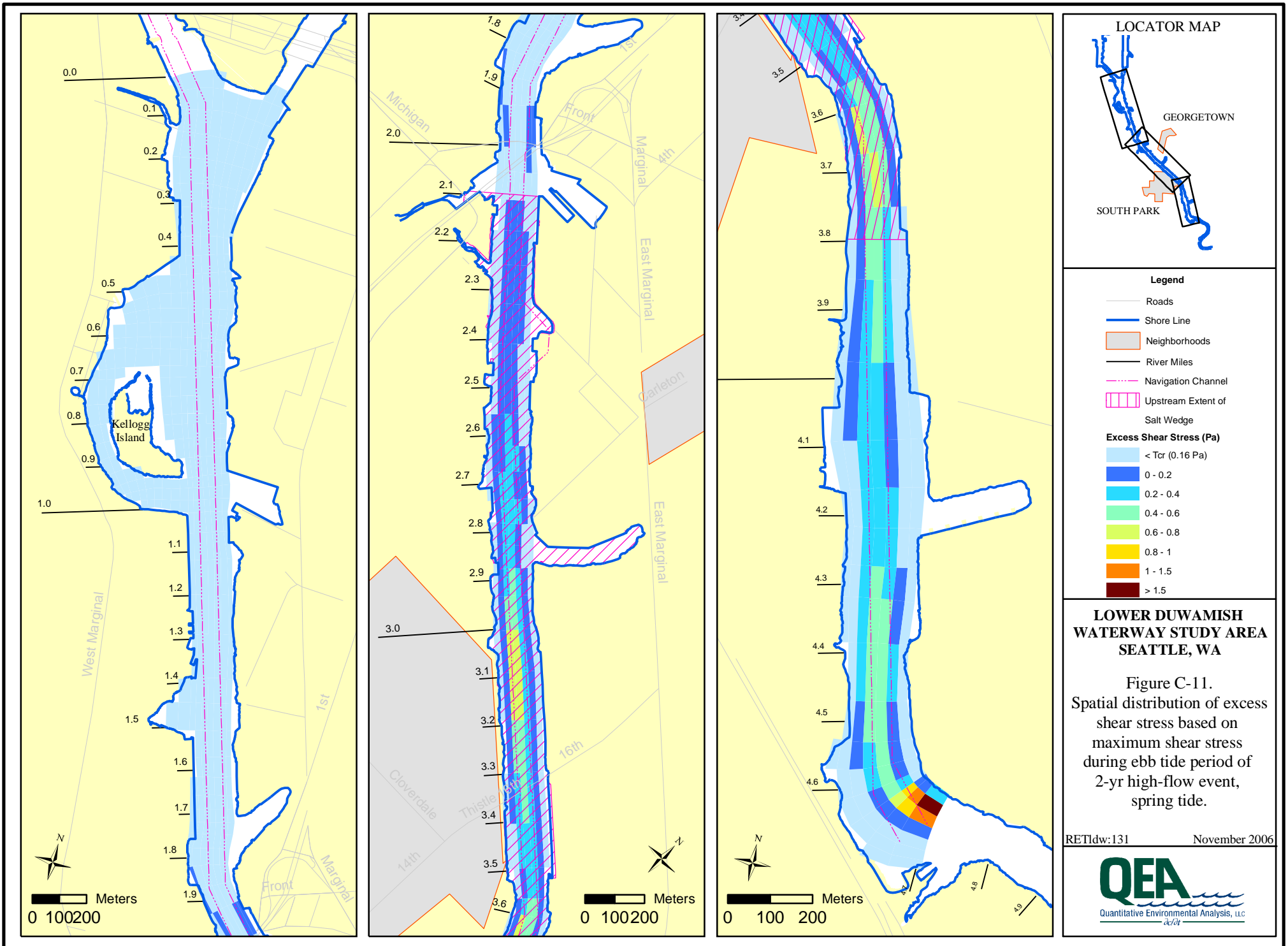
Figure C-8. Spatial distribution of critical shear stress exceedance areas based on maximum shear stress during flood tide period of 2-yr high-flow event, spring tide.

RETIdw:131 November 2006







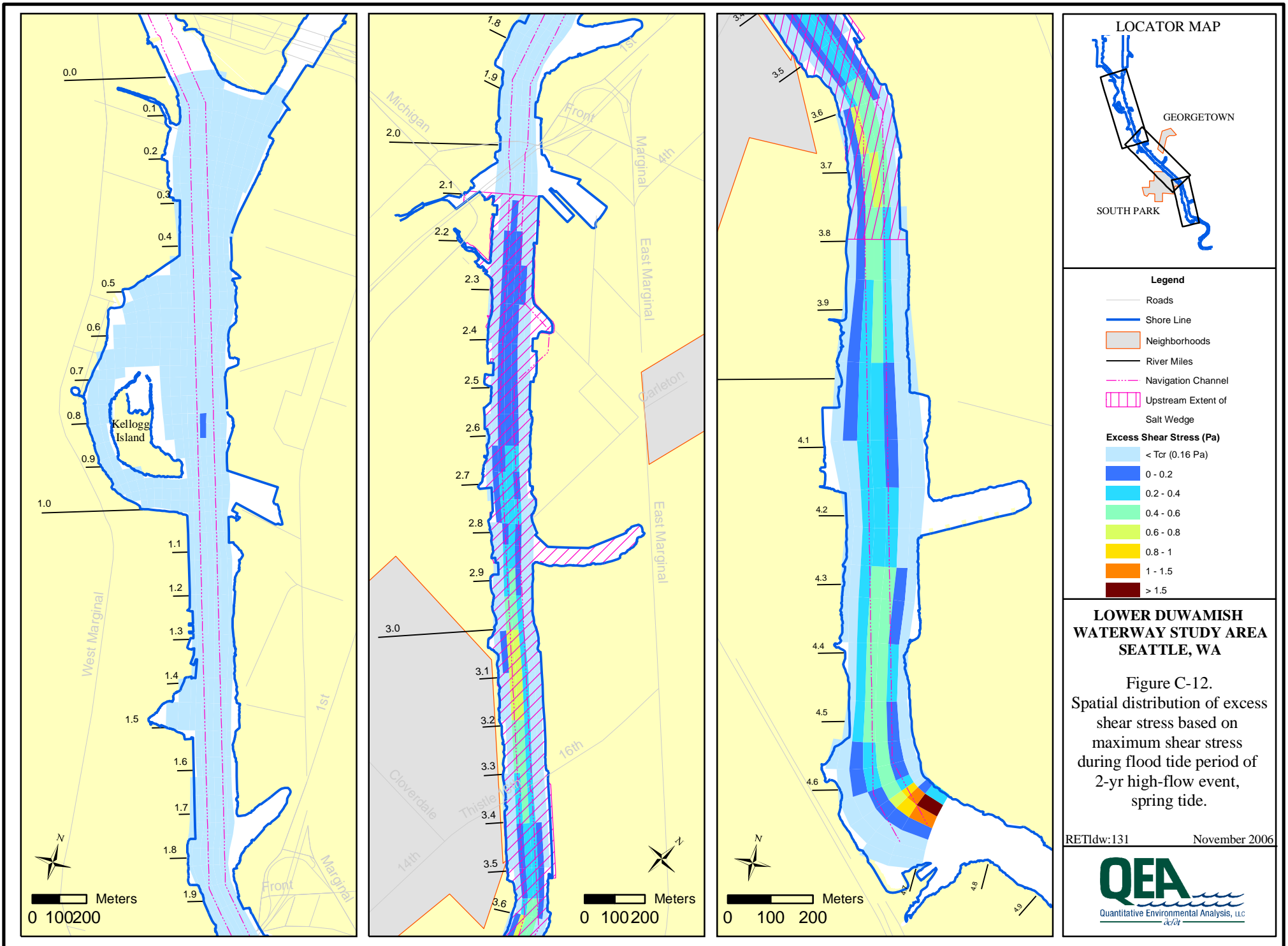


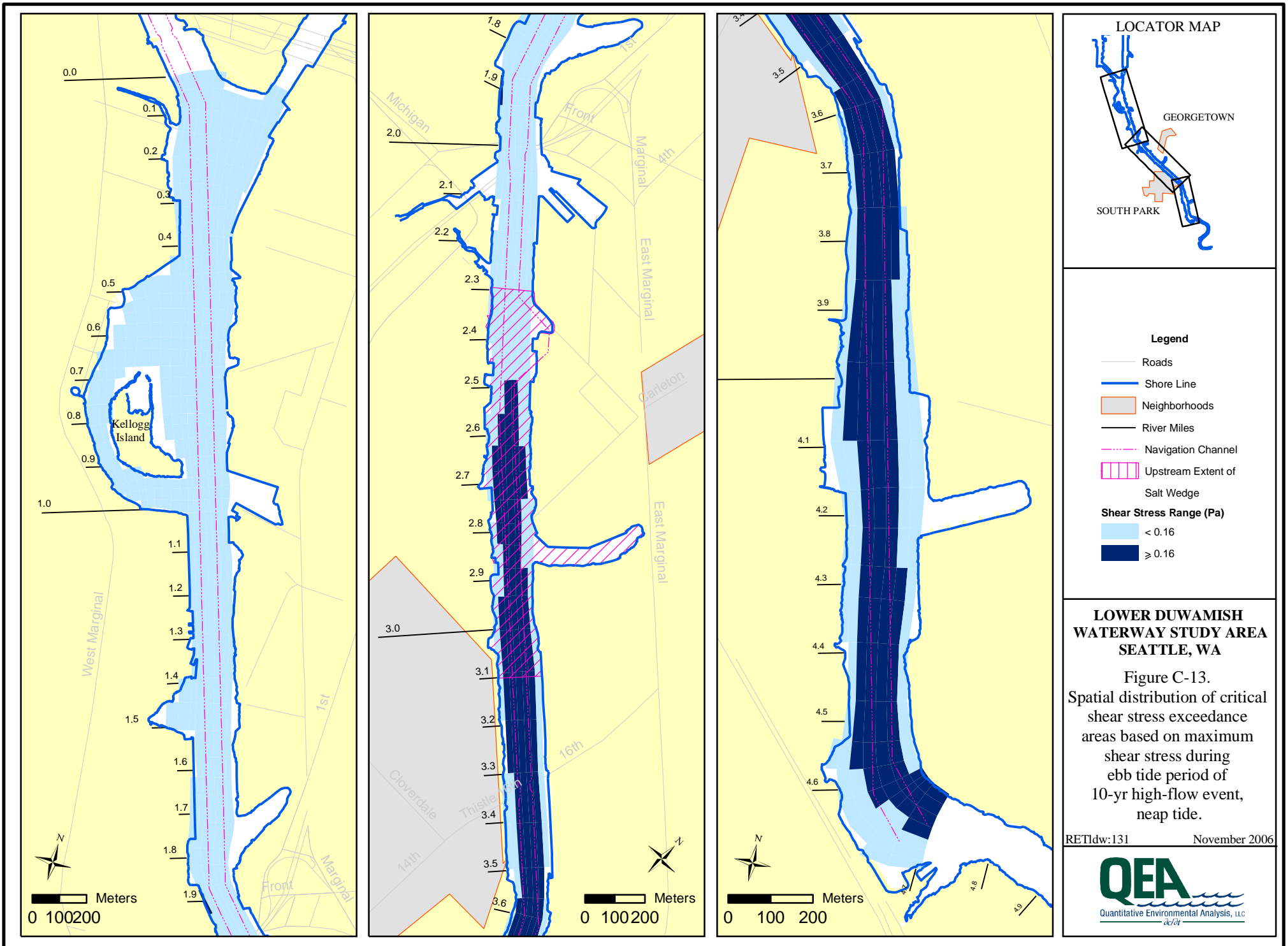
LOWER DUWAMISH WATERWAY STUDY AREA SEATTLE, WA

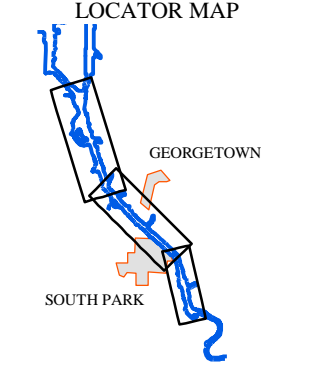
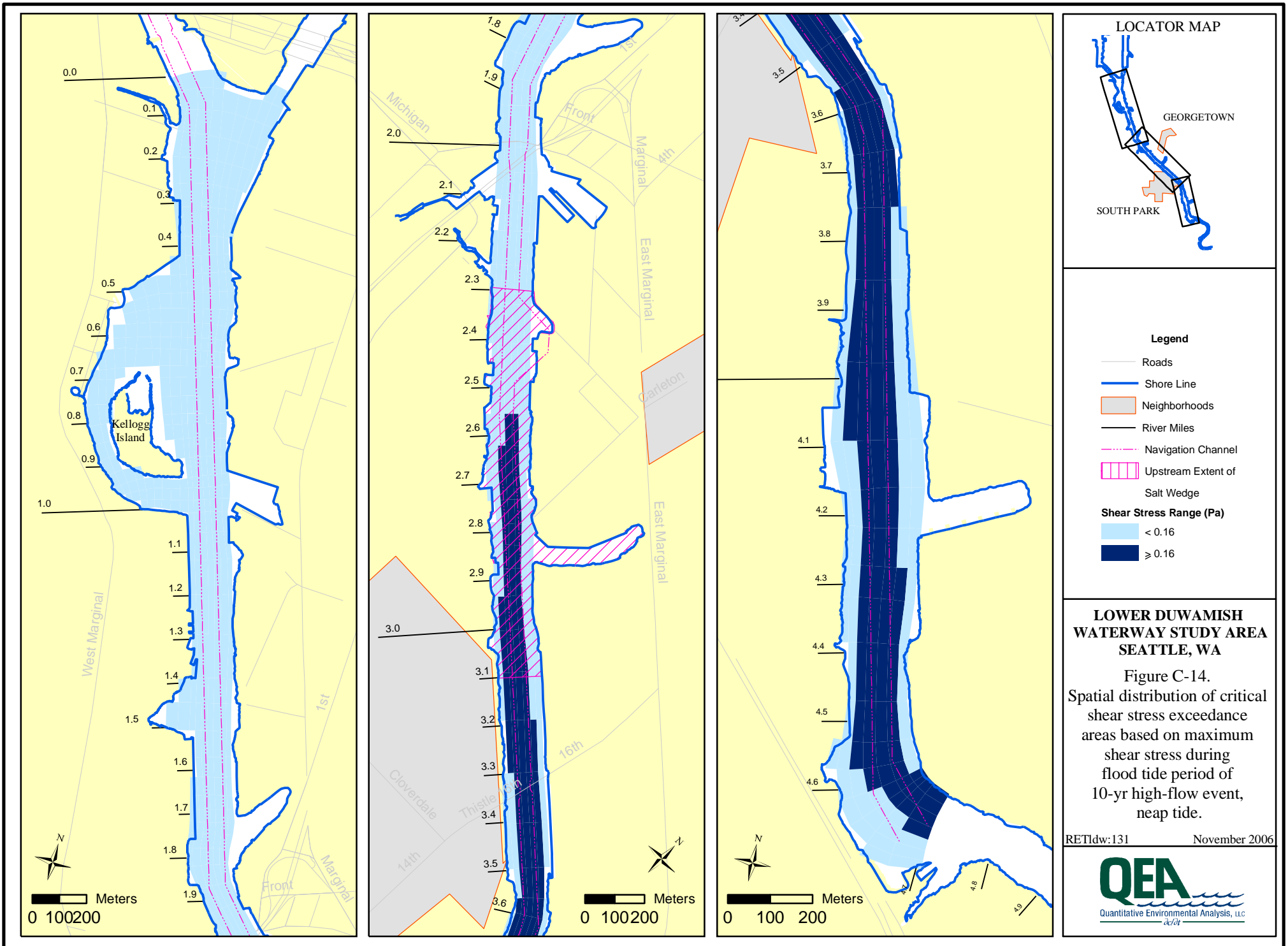
Figure C-11. Spatial distribution of excess shear stress based on maximum shear stress during ebb tide period of 2-yr high-flow event, spring tide.

RETIdw:131 November 2006









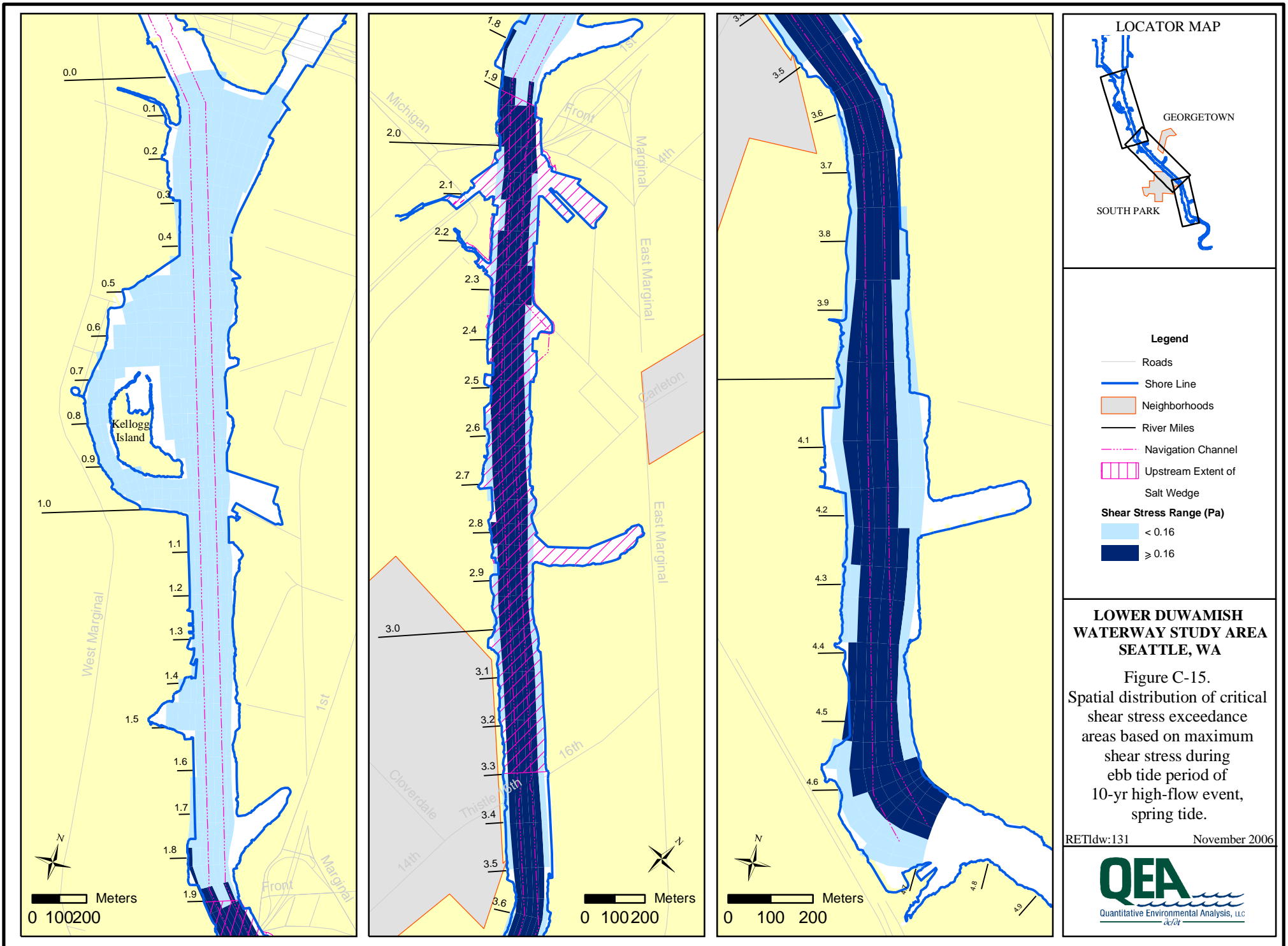
- Legend**
- Roads
 - Shore Line
 - Neighborhoods
 - River Miles
 - Navigation Channel
 - Upstream Extent of Salt Wedge
- Shear Stress Range (Pa)**
- <math>< 0.16</math>
 - ≥ 0.16

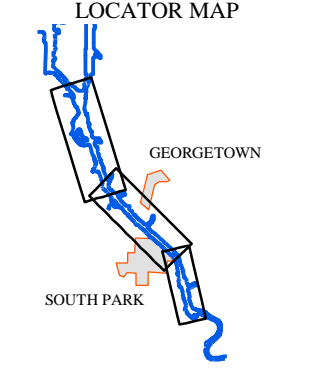
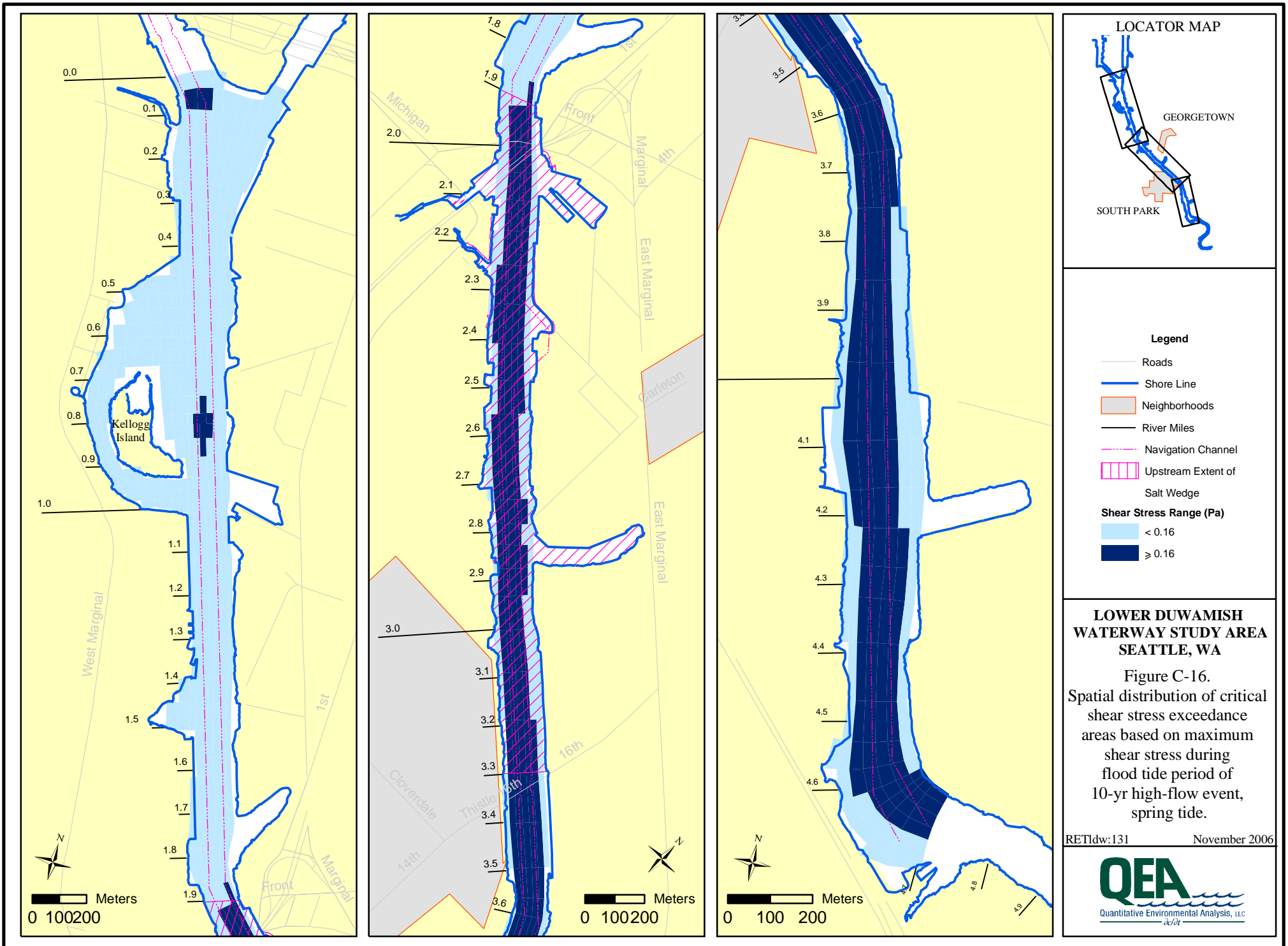
LOWER DUWAMISH WATERWAY STUDY AREA SEATTLE, WA

Figure C-14. Spatial distribution of critical shear stress exceedance areas based on maximum shear stress during flood tide period of 10-yr high-flow event, neap tide.

RETIdw:131 November 2006







Legend

- Roads
- Shore Line
- Neighborhoods
- River Miles
- Navigation Channel
- Upstream Extent of Salt Wedge

Shear Stress Range (Pa)

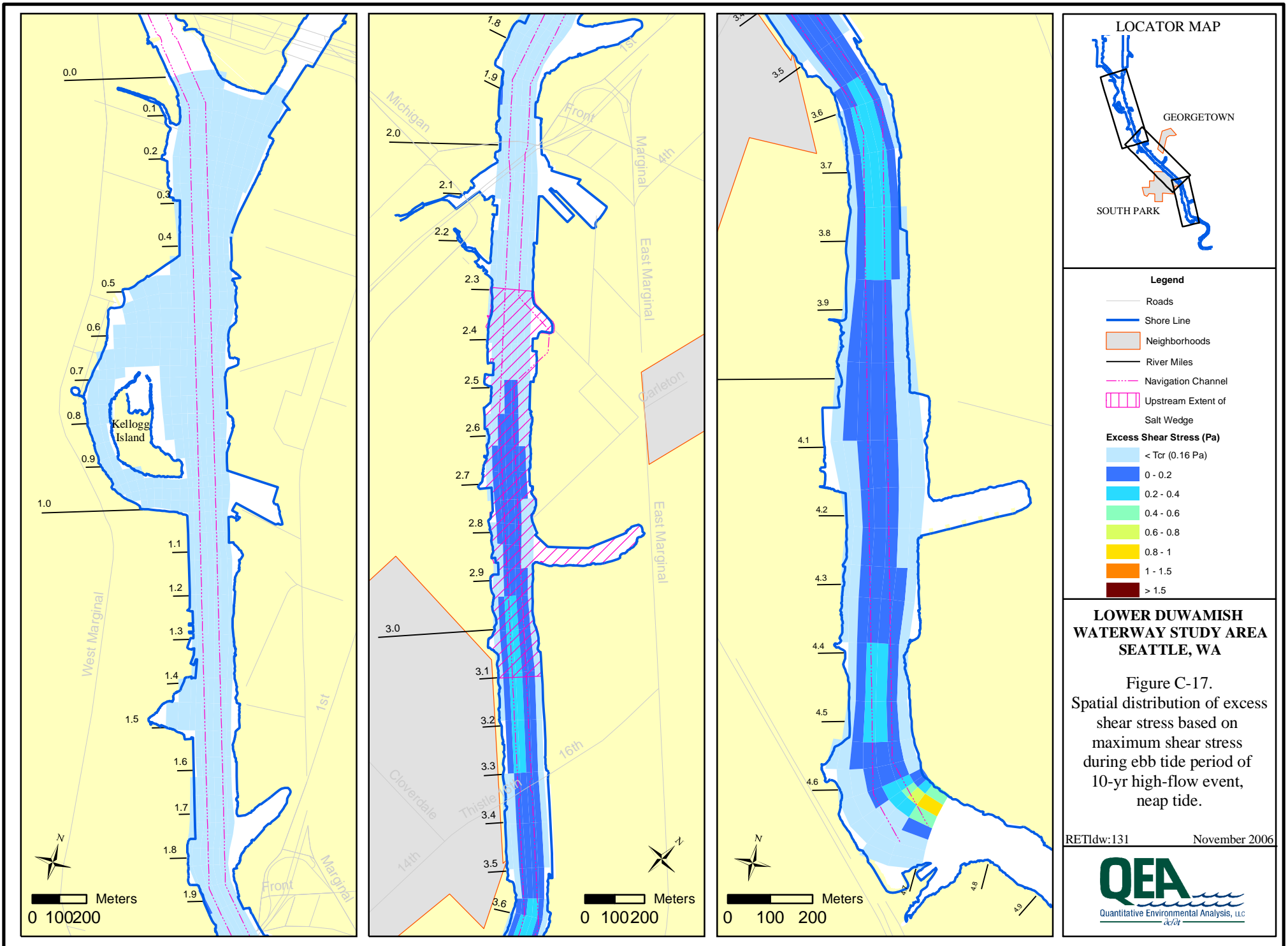
- < 0.16
- ≥ 0.16

LOWER DUWAMISH WATERWAY STUDY AREA SEATTLE, WA

Figure C-16. Spatial distribution of critical shear stress exceedance areas based on maximum shear stress during flood tide period of 10-yr high-flow event, spring tide.

RETIdw:131 November 2006



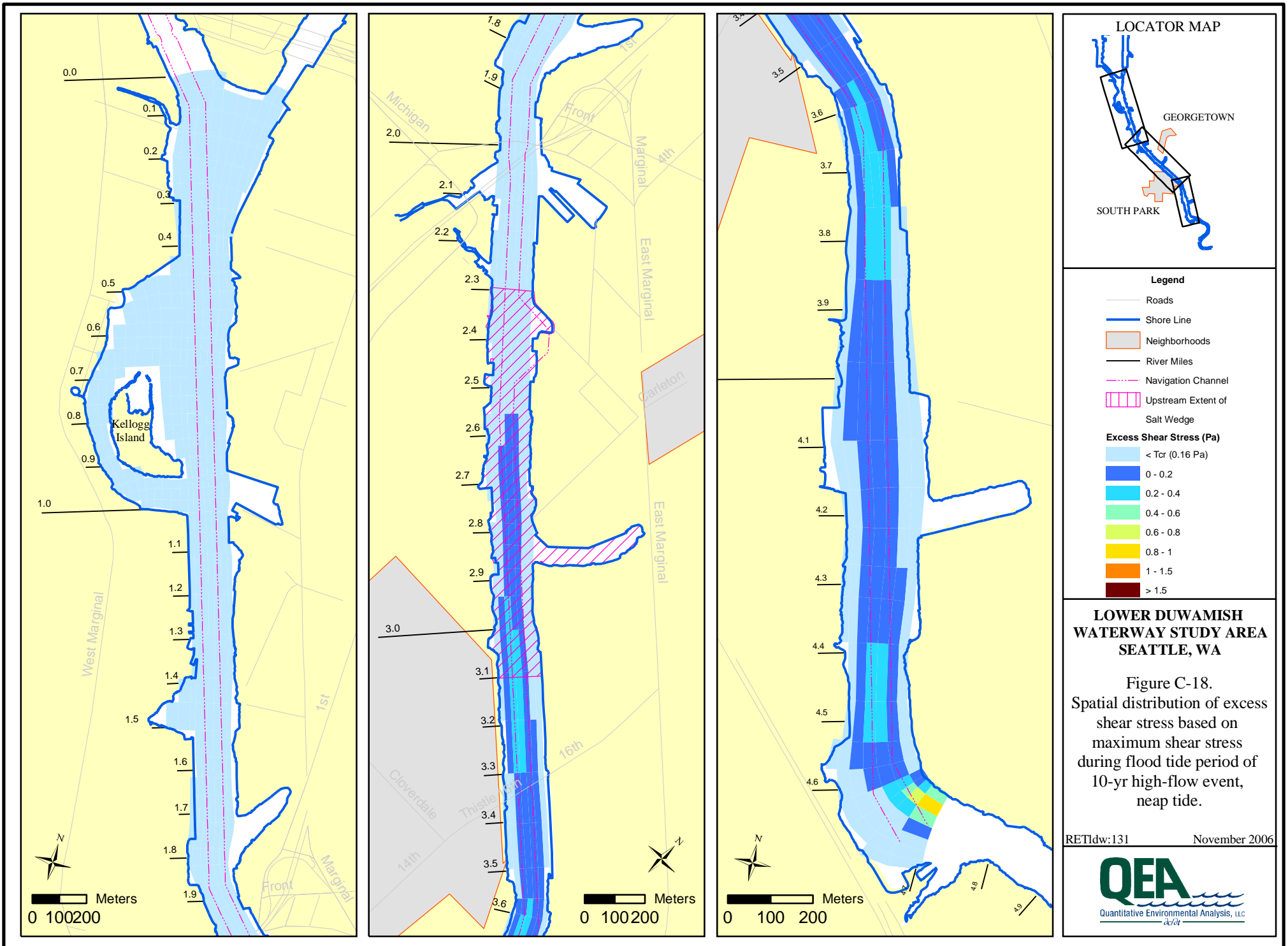


LOWER DUWAMISH WATERWAY STUDY AREA SEATTLE, WA

Figure C-17. Spatial distribution of excess shear stress based on maximum shear stress during ebb tide period of 10-yr high-flow event, neap tide.

RETIdw:131 November 2006



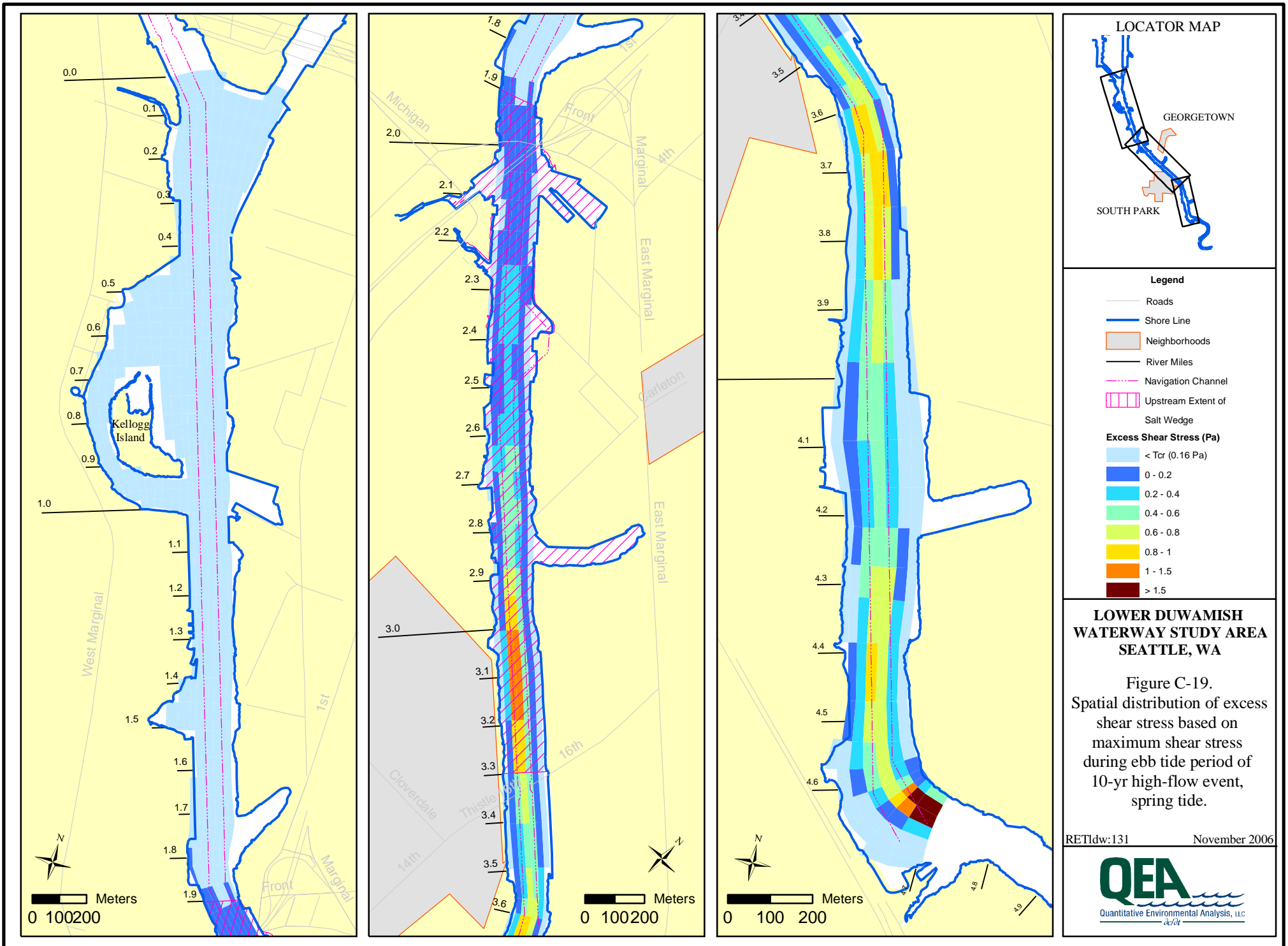


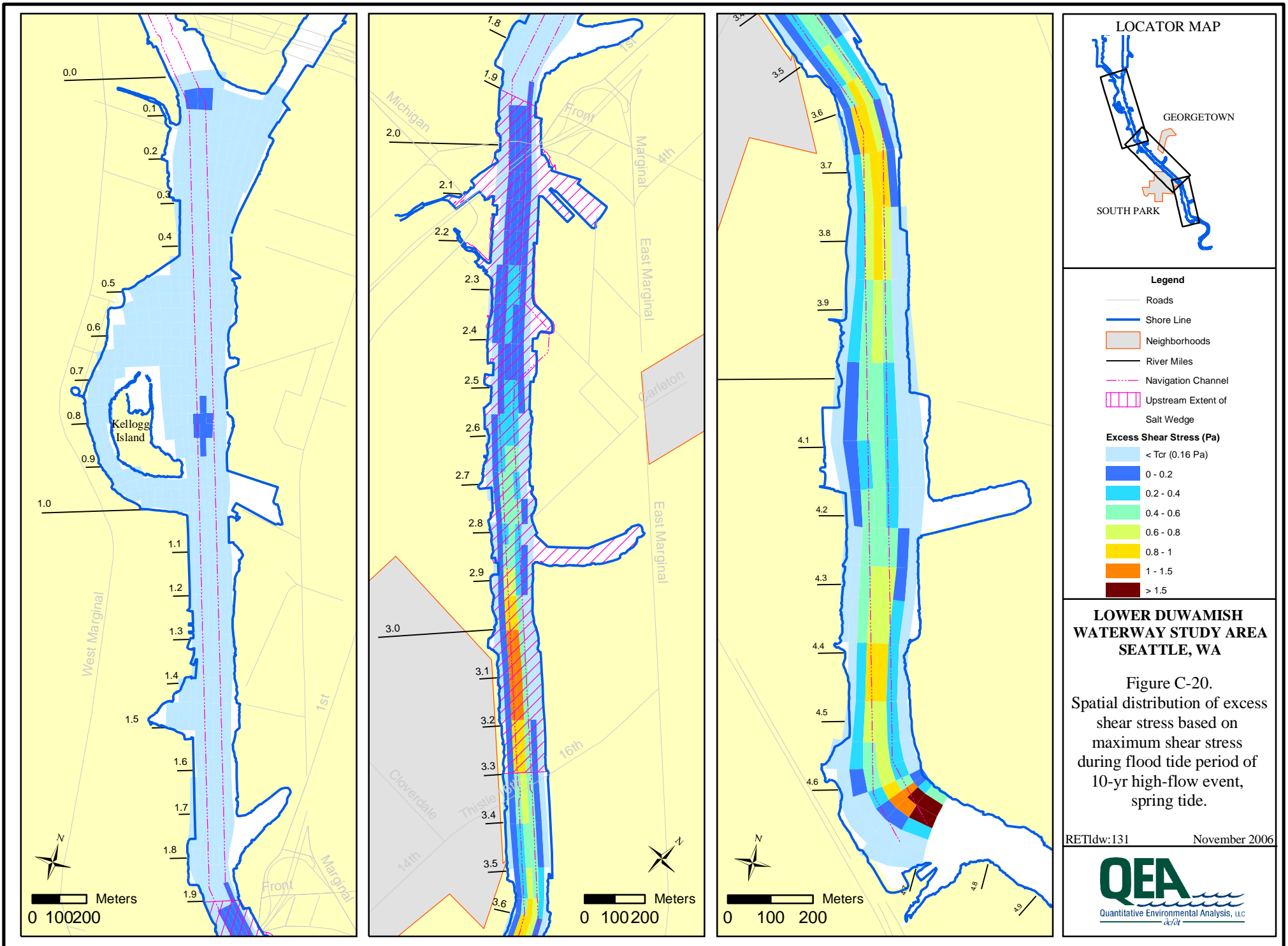
LOWER DUWAMISH WATERWAY STUDY AREA SEATTLE, WA

Figure C-18. Spatial distribution of excess shear stress based on maximum shear stress during flood tide period of 10-yr high-flow event, neap tide.

RETIdw:131 November 2006





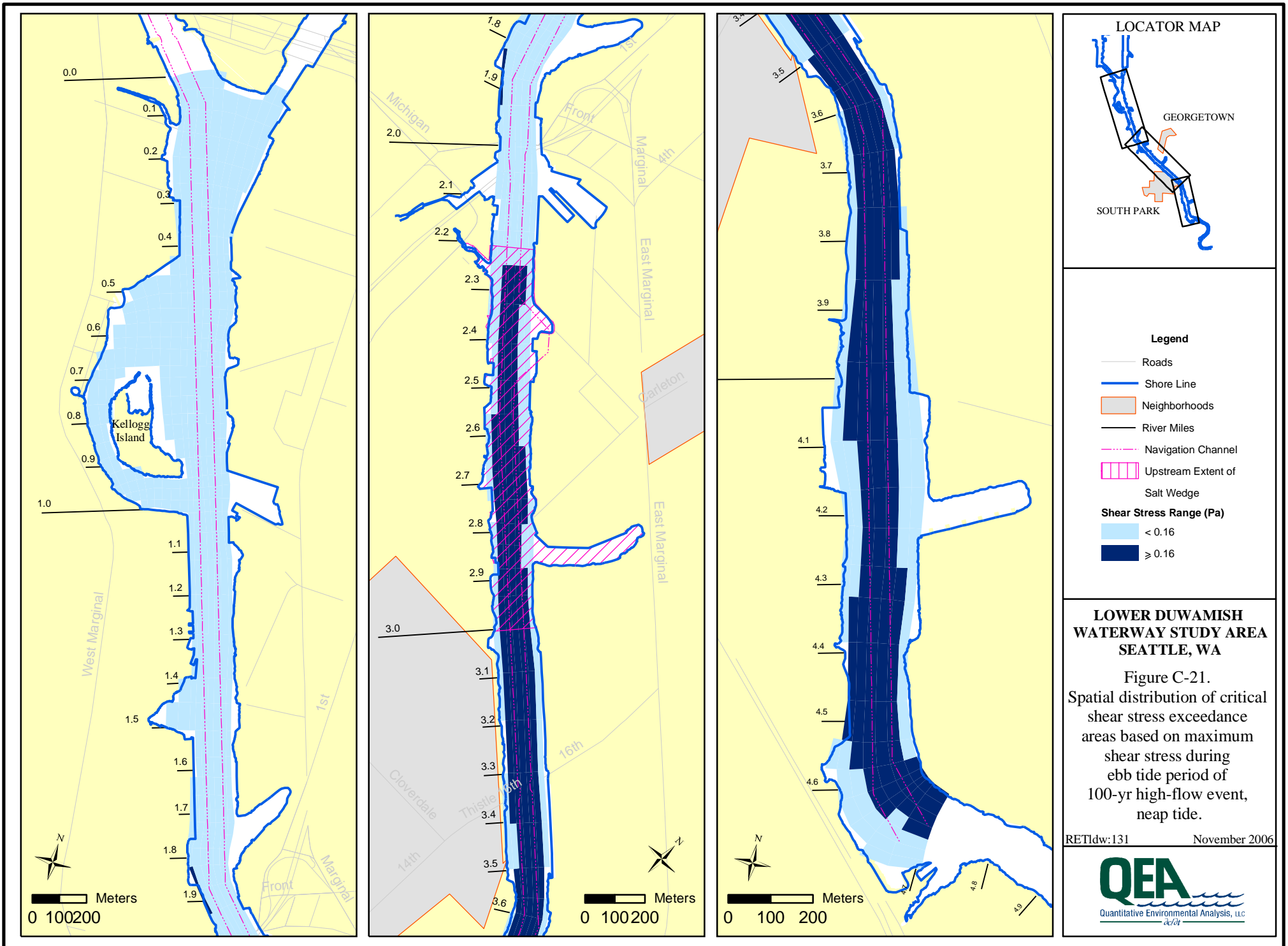


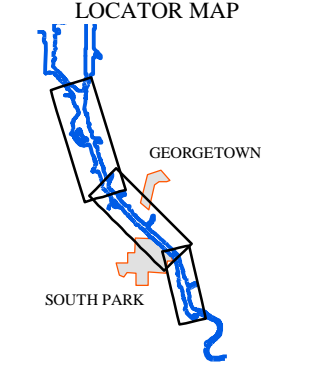
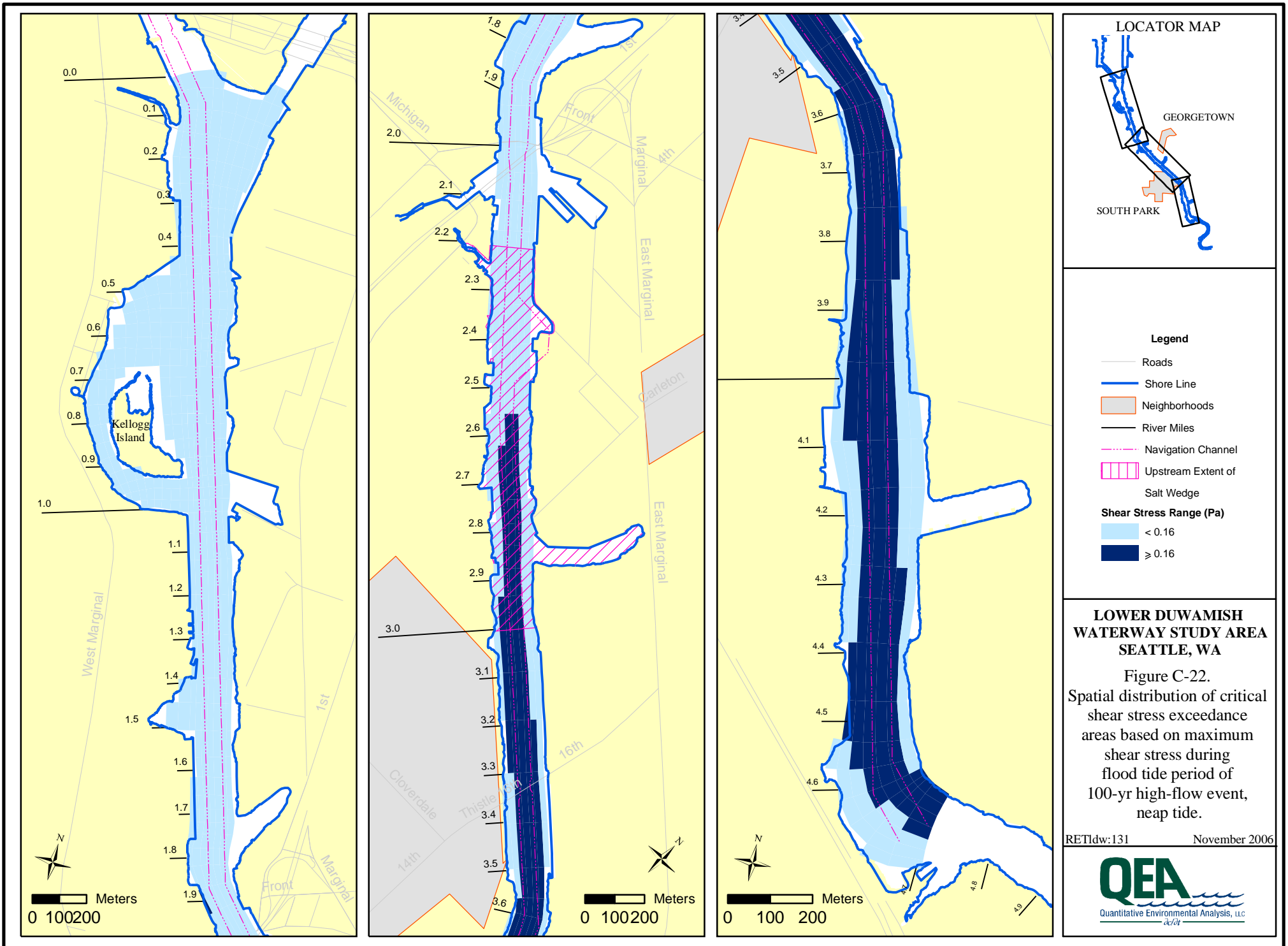
LOWER DUWAMISH WATERWAY STUDY AREA SEATTLE, WA

Figure C-20. Spatial distribution of excess shear stress based on maximum shear stress during flood tide period of 10-yr high-flow event, spring tide.

RETIdw:131 November 2006







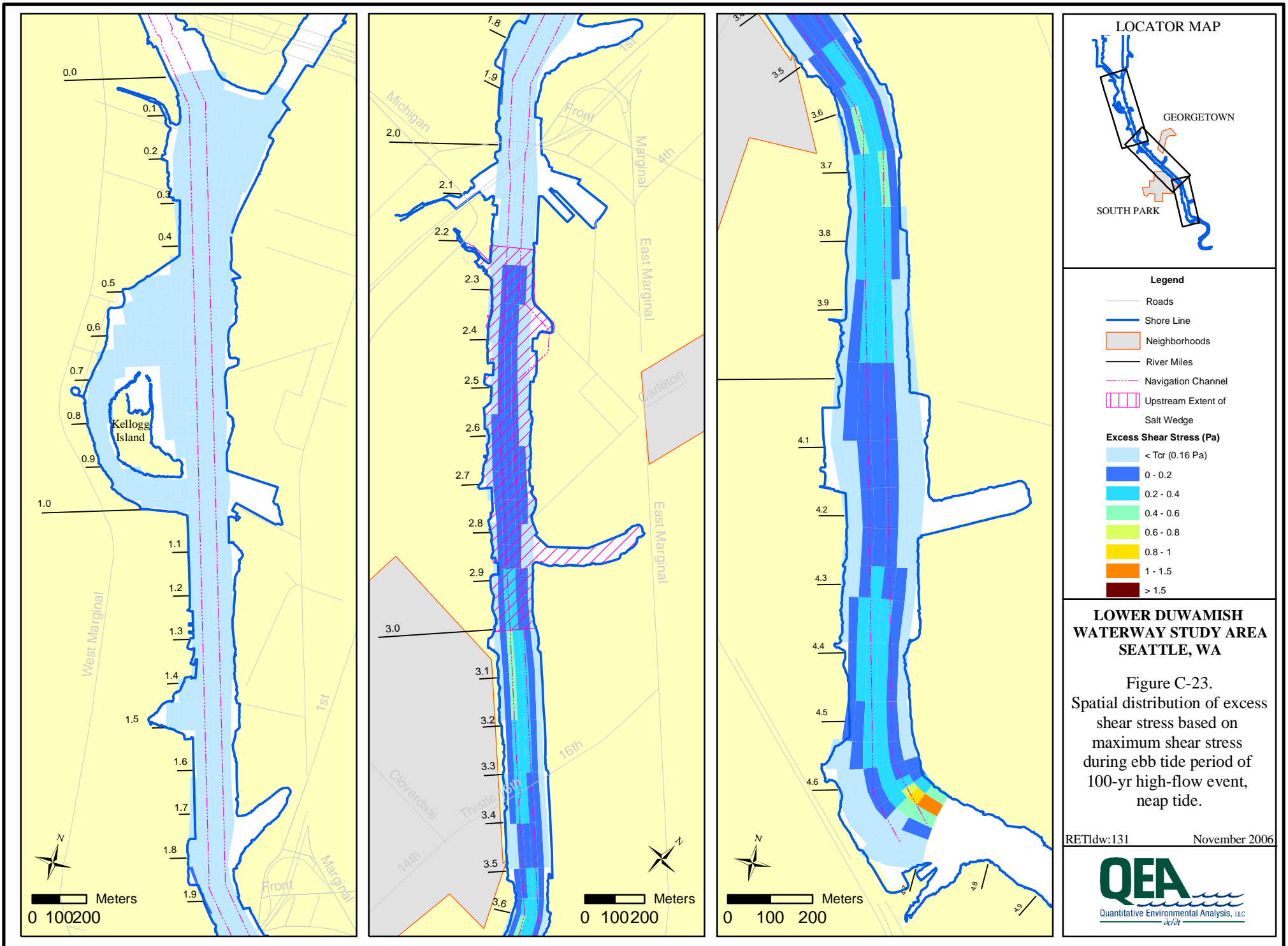
- Legend**
- Roads
 - Shore Line
 - Neighborhoods
 - River Miles
 - Navigation Channel
 - Upstream Extent of Salt Wedge
- Shear Stress Range (Pa)**
- <math>< 0.16</math>
 - >= 0.16

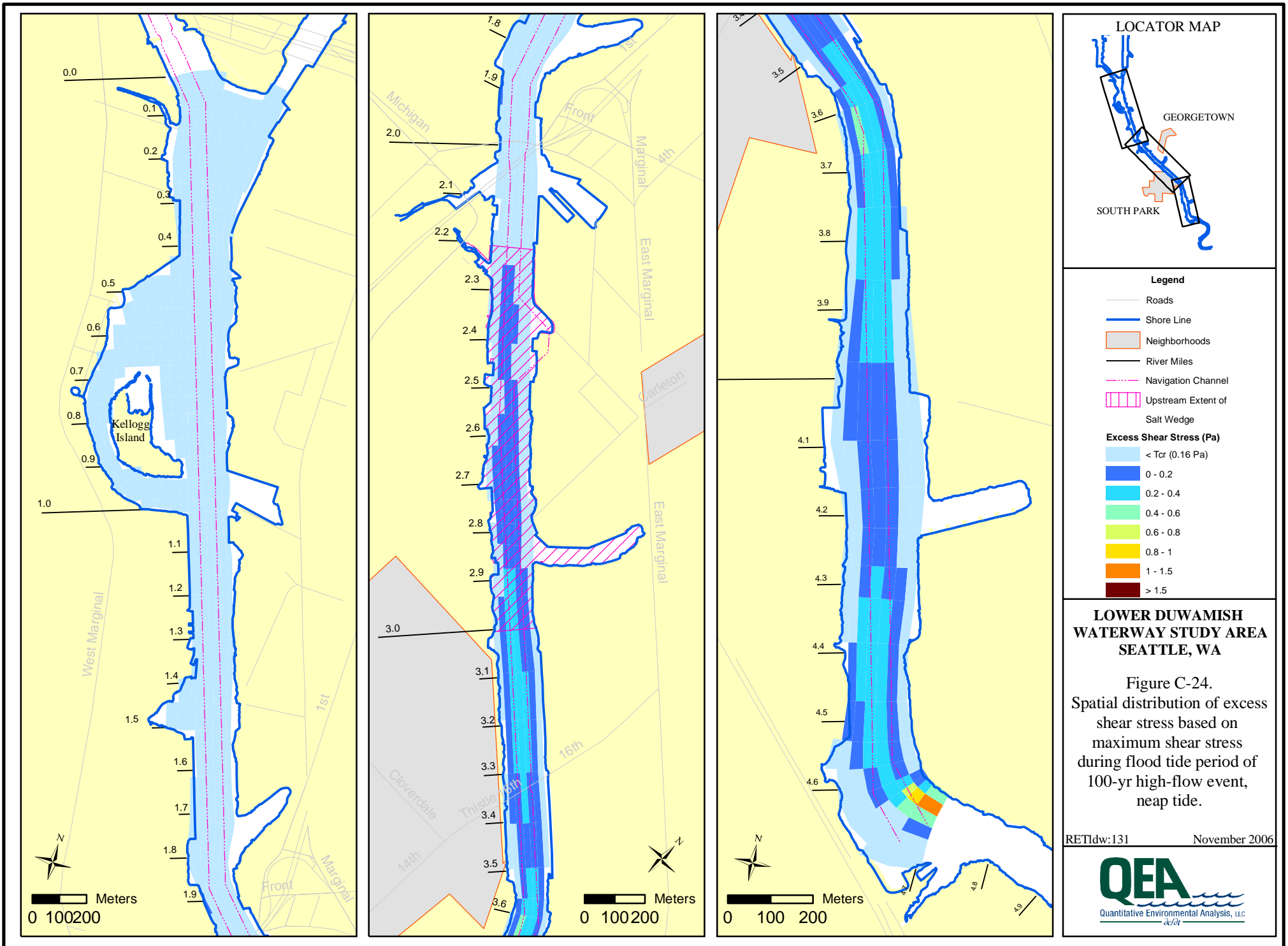
LOWER DUWAMISH WATERWAY STUDY AREA SEATTLE, WA

Figure C-22. Spatial distribution of critical shear stress exceedance areas based on maximum shear stress during flood tide period of 100-yr high-flow event, neap tide.

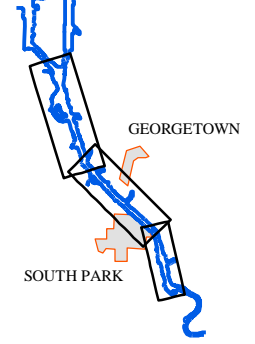
RETIdw:131 November 2006







LOCATOR MAP



Legend

- Roads
- Shore Line
- ▭ Neighborhoods
- River Miles
- Navigation Channel
- ▭ Upstream Extent of Salt Wedge

Excess Shear Stress (Pa)

- <math>< T_{cr}</math> (0.16 Pa)
- 0 - 0.2
- 0.2 - 0.4
- 0.4 - 0.6
- 0.6 - 0.8
- 0.8 - 1
- 1 - 1.5
- > 1.5

LOWER DUWAMISH WATERWAY STUDY AREA SEATTLE, WA

Figure C-24. Spatial distribution of excess shear stress based on maximum shear stress during flood tide period of 100-yr high-flow event, neap tide.

RETIdw:131 November 2006

